IEEE Access
Multidisciplinary | Rapid Review | Open Access Journal

Received January 12, 2020, accepted February 3, 2020, date of publication February 17, 2020, date of current version February 26, 2020.

Digital Object Identifier 10.1109/ACCESS.2020.2974277

Experimental Evaluations of TDD-Based Massive MIMO Deployment for Mobile Network Operators

ENGIN ZEYDAN[1], (Member, IEEE), OMER DEDEOGLU[2], AND YEKTA TURK[3], (Member, IEEE)

[1]Centre Tecnologic de Telecomunicacions de Catalunya, 08860 Barcelona, Spain
[2]Radio Network Planning Department, Türk Telekomünikasyon A.S., 34889 İstanbul, Turkey
[3]Mobile Network Architect, 34889 İstanbul, Turkey

Corresponding author: Engin Zeydan (engin.zeydan@cttc.cat)

This work was supported in part by the Spanish MINECO under Grant TEC2017-88373-R (5G-REFINE), and in part by the Generalitat de Catalunya under Grant 2017 SGR 1195.

ABSTRACT Massive Multiple Input Multiple Output (MIMO) is an essential component for future wireless cellular networks. One of its biggest advantages is to use the 5G spectrum more intelligently by extending both coverage (via high gain adaptive beamforming) and capacity (via high order spatial multiplexing). In this paper, we evaluate the performance of Time-division duplex (TDD)-based massive MIMO deployment scenario in one of the commercial sites in Turkey. Our experimental results reveal three major contributions: (i) TDD-based massive MIMO in 10 Mhz reveals up to 212% and 50% higher cell throughput compared to Frequency-division duplex (FDD)-based MIMO deployments with 10 Mhz and 20 Mhz respectively. The Downlink (DL) throughput is also observed to be better in mid/far points. (ii) Together with the usage of TDD-based massive MIMO inside the same commercial site, median values of total cell traffic, Uplink (UL) Spectral Efficiency (SE) and DL schedule Transmission Time Interval (TTI) duty cycle have improved 38%, 9% and 14.5% compared to FDD-based MIMO scenario respectively. (iii) Finally, we address some of the challenges of the massive MIMO deployments and the possible trade-offs that can be observed in terms of Radio Resource Control (RRC)-connected User Equipments (UEs), cell throughput, available Sounding Reference Signal (SRS) resources and pairing opportunities provided by massive MIMO.

INDEX TERMS Experiments, massive MIMO, measurements, real-world testbed, TDD, FDD.

I. INTRODUCTION

The race to 5G deployments is heating up and brand new 5G technologies are beginning to become reality on top of Mobile Network Operators (MNOs)' infrastructures [1]. In fact, 5G will be implemented with several diverse technologies including massive Multiple Input Multiple Output (MIMO), Internet of Things (IoT), millimeter wave (mmWave), Device-to-Device (D2D) communication and Ultra Dense Networks (UDNs). On the other hand, MNOs still face the need to acquire more capacity over their acquired spectrum to accommodate the ever-increasing number of users and their bandwidth demands. It is predicted that billions of devices will be connected with 5G but there is still a limited frequency spectrum [2]. As the number of users increases, the network has to schedule the users in an appropriate way under resource constraint environment to keep high quality-of-service (QoS) and fairness levels for all users. Due to this non-optimal situation, a real network in a resource-limited region cannot provide the desired resources to all users at the same time. Consequently, the overall throughput could reduce. However, as the spectrum band of 5G is increasing to above 1 Ghz, the size of the antenna elements can become smaller. This can enable the possibility to fit higher number of such antenna elements into a space. Using much higher numbers of antennas would allow to handle large number of users in an efficient and reliable manner [3].

Together with more radios operating at higher frequency bands and availability of adequate transmit power, a massive MIMO system could significantly advance both the range

The associate editor coordinating the review of this manuscript and approving it for publication was Meng-Lin Ku.

of operation and capacity compared with single antenna systems [4]. In massive MIMO systems, huge number of antennas can be used coherently (via beamforming) to increase the gain of the transmitted signals, thereby emitting less power when transmitting data and creating a more energy efficient system [5]. Therefore, massive MIMO together with beamforming can help to build future networks that are robust enough so that future services and products such as autonomous cars, factories of future, Virtual Reality (VR) applications can rely on. Previously in both 3G and Long Term Evolution (LTE) networks, MIMO technology has been implemented with up to eight antenna elements that are placed at Base Stations (BSs) (or transmitters) and four at receivers. Massive MIMO on the other hand, utilizes coordinated antenna elements to serve multiple users simultaneously via relatively simple scheduling and receiver algorithms that will allow multiple signal beams to be directed towards users. This also enhances coverage while providing better indoor penetration. Therefore, it is a core technology for 5G which promises an advanced networking capability.

Typically, massive MIMO can bring huge benefits to MNOs on IMT-2020 defined use cases such as Enhanced Mobile Broadband (eMBB) in terms of providing more bandwidth and Machine-Type of Communications (MTC) and Ultra-Reliable Low-Latency Communication (URLLC) in terms of letting more user connectivity in a reliable manner. These can increase user experience and encourage users to consume more data. Recently, massive MIMO has been in the interest of industry due to its potential as being a key element of 5G New Radio. It uses simultaneous transmit and receive streams and creates much higher network capacity when compared to typical MIMO that uses two transmit and receive antenna elements to double the capacity. Compared to LTE BSs, the capacity of mobile networks can be increased by a factor of 22 or greater with massive MIMO [6].

In a typical $H \times R$ MIMO where H denotes the number of logical channels and R denotes the number of receivers, MIMO efficiency is limited by $min(H, R)$. Fundamentally, massive MIMO can be described as having multiple independently controlled antenna elements at the BS for beams to concentrate the radio energy to a single location. Users in that location receive higher quality radio signals and experience higher data rates. Additionally, unwanted radio energy or interference is also minimized because the access attempts from the other channels are minimized as well. For example, massive MIMO with 64T64R can provide 3 times higher capacity gain and 8dB more coverage gain compared to 8T8R in urban scenarios [7]. Hence, massive MIMO is a significant enabler for deployment of Gigabit LTE and 5G systems for MNOs.

There are basically two different massive MIMO practical deployment strategies, Frequency-division duplex (FDD) and Time-division duplex (TDD)-based massive MIMO. TDD-based massive MIMO is considered to be a major step towards 5G evolution [8]. The main benefits comes with increased capacity and speed while using the same amount of spectrum. Massive MIMO provides a capacity boost in hot-spot locations of networks, so that MNOs can deliver high speed services and better quality to their end-users. Therefore, applications that need high bandwidth such as High Definition (HD) VR, 6K and 8K TV in those regions can easily be sustainable with massive MIMO.

However, massive MIMO technology also requires important considerations when design, optimization and large-scale deployments are done in practical systems and commercial networks. In this paper, we study a real-world massive MIMO deployment scenario where both Single-User (SU) FDD-based MIMO and TDD-based massive MIMO deployments are used. Our analysis is based on measuring and comparing different Key Performance Indicators (KPIs) that are collected for six days from a real experimental test site, in Turkey. We also use our experimental results to observe various benefits and possible trade-offs of utilizing both traditional MIMO with higher bandwidth and massive MIMO deployment strategies.

The rest of the paper is organized as follows: Section II provides the related work the main contributions of the paper. Section III presents the system model and concepts related to massive MIMO and also includes a subsection that provides a general overview of massive MIMO deployment strategies. The experimental results and discussions on general deployment issues that need to be considered are presented in Section IV. Finally in Section V, we provide the conclusions and future works of the paper.

II. RELATED WORK AND MOTIVATION

Massive MIMO is considered to be one of the most efficient and effective approach for MNOs to increase their network capacity [9]. It has been a reality in many commercial systems that are deployed in many countries [10]. Commercial equipment supporting Massive MIMO are being driven on the market as of today and the features of the devices are being developed over time [11], [12], [13]. It is also playing a key role in terms of providing coverage to large regions and serving User Equipments (UEs) that are moving fast. The authors in [10] have outlined five new massive MIMO related research directions including large-scale MIMO radar, extremely large aperture arrays, six-dimensional positioning, intelligent and holographic massive MIMO. A tutorial article towards massive MIMO 2.0 in [14] demonstrates the existence of unlimited theoretical capacity of massive MIMO by considering naturally existent spatial propagation channel correlation and signal processing schemes that suppress both intra-cell and inter-cell interference. The article in [15] modeled and compared the techo-economic aspects of Massive MIMO in terms of capital expenditure (CapEx) and operating expenditure (OpEx).

In the context of massive MIMO deployments in industry, different MNOs have started first deployments of TDD-based LTE with massive MIMO functionality. US carrier Sprint has launched BSs with massive MIMO capabilities in different cities such as Chicago, Dallas, and Los Angeles on

April 2018 [16]. In comparison to LTE, the increase in network capacity has been trialed to be up to 10 times together with the deployment of 5G massive MIMO [17]. Similarly, Verizon launched its first FDD-based massive MIMO deployment trial back in December 2017 [18]. O2 in UK is launching 5G-focused massive MIMO trial in London [19]. The expected overall improvements of spectral efficiency using massive MIMO can be 20x to 40x compared to International Mobile Telecommunications (IMT) Advanced requirements [20], [21].

Experimental comparisons between FDD and TDD for beamforming performance are tested in [22] at 2.6 Ghz, which prove better performance is achieved with the usage of TDD. Another real-time experimental test in a software-defined radio based test-bed with number of BS antennas up to 100 or higher is presented in [23]. The authors in [23] have also demonstrated a framework for designing real-time testbed for massive MIMO implementation. However, the number of UEs utilized during the test-bed evaluation is limited. In [24], the authors perform field trials with 128 antenna elements, however the test includes only 6 users. Gao et al. in [25] investigated how massive MIMO performs in channels measured in real propagation environments at 2.6 GHz using a virtual uniform linear array and a practical uniform cylindrical array, both having 128 antenna ports. The experimental study in [26] investigated the practical performance of MU massive MIMO systems with linear and non-linear downlink precoding schemes. An analysis of the ergodic achievable rate of an Uplink (UL) massive MIMO system with a large and Poisson distributed number of users is studied in [27].

A comparison of massive MIMO with polar code against turbo code in a large-scale 5G field trial with a system that works 64 antennas and 200 MHz bandwidth is presented in [28]. The study in [29] presents a design approach for the TDD-based 128-antenna massive MIMO prototype system from theory to reality. The article in [29] focused on two concepts, an analytic signal model and a link-level simulation consistent with practical TDD-based massive MIMO systems. The paper in [30] have considered performance of two different scenarios for pilot signals allocation in TDD multi-cell massive MIMO systems. In [31], the authors performed a channel calibration method and proposed an analysis on the accuracy of the channel state information at the transmitter in a massive MIMO TDD system. In [32], the use of massive MIMO and small cell access point (SCA) approaches for power optimization are combined and the effect of FDD and TDD techniques on power optimization performance are evaluated.

There are many existing properties and features of massive MIMO that brings potential benefits to users and operators of the systems from different aspects. These aspects cover research directions towards spectral efficiency analysis [33], power optimization and pilot contamination analysis [34], channel estimation and interference alignment methods [35]–[37]. For example, it is known that both TDD and FDD-based massive MIMO systems have the ability to extend cell-edge coverage. To accomplish this, Interference Alignment (IA) methods can be used to enhance the transmission capabilities for cell-edge users. Moreover, a Soft-Space-Reuse (SSR) based scheme can be utilized with allocation of low-level power transmission to the cell-center users in multi-cell massive MIMO systems as proposed in [37]. FDD-based MIMO systems in general (either in SU, Multi-User (MU) or massive MIMO scenarios) are known to exhibit significant pilot and feedback overhead for channel state information (CSI) acquisition purposes. To mitigate the inefficiency of resulting high feedback overhead of FDD-based systems, the authors in [38] have designed FDD-based large-scale MIMO systems utilizing limited feedback and pilot overhead. Moreover, the authors in [39] have shown that together with appropriate choice of investigated eigenspace channel estimation schemes that exploit spatial channel correlation, the achievable rate gap between FDD and TDD-based massive MIMO systems can be narrowed down.

In the literature, there are also various theoretical solutions that concentrate on application of performance enhancement techniques that are applicable to both TDD and FDD based massive MIMO systems [35], [36]. The authors in [35], [36] have worked mostly on theoretical approaches for Downlink (DL) and UL channel estimation schemes to improve the efficacy of system and channel tracking performance in massive MIMO systems. In [35], a unified UL/DL channel estimation and scheduling strategy is proposed where the antenna elements of massive MIMO systems at the BS can concentrate spatial beams towards the users. Similarly, a learning based approach for UL and DL channel estimation of time varying parameters of massive MIMO channels for both FDD and TDD-based schemes are studied in [36].

Most of the literature works described above on massive MIMO deployment scenarios include either theoretical analysis and/or simulation results. These results either lack real-world experimental trials when comparisons with traditional MIMO scenarios with different bandwidth utilization are observed or consider deployment scenarios with very small number of test-users that lack realistic large-scale observation conditions. Compared with the above existing works, in this paper we study real-world experimental trial of TDD-based massive MIMO and compare its KPI performances with traditional FDD-based MIMO deployments in various bandwidth utilization to observe its benefits and gains. The experimental tests are done via observing real-users performance results on a commercial site based in Turkey. Our experiments results are also evaluated in terms of existence of possible trade-offs for future massive MIMO deployment scenarios.

Main Contributions: This paper shows experimental analysis of massive MIMO trial focusing on TDD-based deployment using one of the telecommunication operator's infrastructure over a commercial site based in Turkey. In particular, we compare TDD-based massive MIMO and higher bandwidth FDD-based MIMO deployments to observe their

KPI differences where the benefits of TDD-based massive MIMO are demonstrated and also several observations are made on describing the involved trade-offs regarding the performance gains. We compare TDD-based massive MIMO with FDD-based MIMO deployments in consecutive one week intervals. Our performance comparisons are done at a single BS that is equipped with both a large massive MIMO antenna array and small scale MIMO antennas. Our contributions in this paper are summarized as follows:

- Performing analysis on real world experimental set-up to observe the performance differences of TDD-based massive MIMO and higher bandwidth FDD-based MIMO deployments on a commercial site based in Turkey.
- Revealing up to 212% and 50% performance benefits in terms of DL cell throughput of TDD-based massive MIMO in 10 Mhz bandwidth compared to FDD-based MIMO in 10 and 20 Mhz bandwidths respectively and better DL throughput in mid/far points.
- Improving the median values of total cell Packet Switched (PS) traffic, UL Spectral Efficiency (SE), DL schedule Transmission Time Interval (TTI) duty cycle by 38%, 9%, 14.5% respectively together with using TDD-based massive MIMO compared FDD-based MIMO scenario in the same commercial site.
- Addressing the possible trade-offs of massive MIMO deployments compared to higher bandwidth FDD-based MIMO deployments that can be observed in terms of user distributions, Radio Resource Control (RRC)-connected UEs, cell throughput, available Sounding Reference Signal (SRS) resources and pairing opportunities.

Notation: The mathematical notations $\mathbf{X}$, $\mathbf{x}$ and x denote a generic matrix, vector and scalar respectively, $\mathcal{C}^{N\times M}$ denotes the set of complex valued $N \times M$ matrices, $\mathbf{A}^H$ is the conjugate transpose of matrix $\mathbf{A}$, $\mathcal{CN}(x, X)$ is the complex Gaussian distribution with mean x and correlation matrix X.

III. SYSTEM MODEL AND CONCEPTS

We assume that the access network involves B BSs with massive MIMO BSs and each equipped with M antennas. There are K_b UEs with N antennas in each BS $b \in \{1, \ldots, B\}$ where M is much larger than K_b, which are spatially multiplexed onto the same time-frequency resource. The channel response vector between UE-k in BS b is denoted by $\mathbf{h}_k^b \in \mathcal{C}^{M\times N}$ where each element corresponds to channel response from UE to BS b with M antennas. Let $\mathbf{y}^b \in \mathcal{C}^{N\times 1}$ be the received signals vector where $\mathbf{y}^b = [\mathbf{y}_1^b, \mathbf{y}_2^b, \ldots, \mathbf{y}_{K_b}^b]^T$. The signal s_k^b intended for UE-k can be decoded using the following received signal,

$$\begin{aligned}\mathbf{y}_k^b &= \sum_{b=1}^{B}(\mathbf{h}_k^b\mathbf{x}^b) + \mathbf{n}_k^b \\ &= \sum_{b=1}^{B}\sum_{i=1}^{K_b}(\mathbf{h}_k^b\mathbf{w}_i^b s_i^b) + \mathbf{n}_k^b \\ &= (\mathbf{h}_k^b)^H\mathbf{w}_k^b s_k^b + \sum_{\substack{m=1\\m\neq b}}^{B}\sum_{\substack{i=1\\i\neq k}}^{K_b}(\mathbf{h}_i^m)^H\mathbf{w}_i^m s_i^m + \mathbf{n}_k^b, \\ &\forall k \in \{1,\ldots,K_b\}, \forall b \in \{1,\ldots,B\} \end{aligned} \quad (1)$$

where BS b transmits the signal $\mathbf{x}^b \in \mathcal{C}^{M\times 1}$ where $\mathbf{x}^b = \sum_{i=1}^{K_b}\mathbf{w}_i^b s_i^b$ and pre-coding vectors $\mathbf{w}_k^b \in \mathcal{C}^{M\times 1}$ satisfy $\mathcal{E}\{||\mathbf{w}_k^b||^2\} = 1$ and $\mathbf{n}_k^b \sim \mathcal{CN}(0, \sigma_{DL}^2)$ is the independent additive receiver noise with variance σ_{DL}^2. We assume that the network operates in TDD mode and the propagation channel between BS-b and UE-k is represented by $\mathbf{h}_\mathbf{k}^\mathbf{b}(t)$ in the t-th timeslot. In most of the works in the literature, the propagation channel $\mathbf{h}_\mathbf{k}^\mathbf{b}(t)$ is generally agreed on to be reciprocal [40].

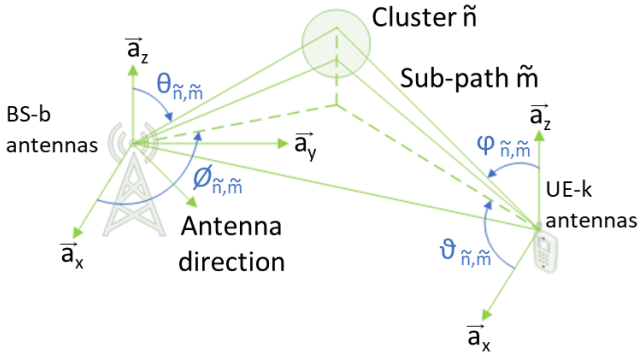

FIGURE 1. 3GPP study on 3D propagation channel modeling environment.

There have been various works in 3rd Generation Partnership Project (3GPP) to characterize the 3D Full Dimension (FD)-MIMO (which can be considered as the practical implementation of massive MIMO system [41]) channel model over the years as in 3GPP TR 36.873 [42]. This channel model is stochastic and formed based on geometry. The 3D Standard Channel Model (SCM) is a composite of $\tilde{N}$ propagation paths which is referred as $\tilde{n}$-th cluster. Angle of Departure (AoD) $(\phi_{\tilde{n}}, \theta_{\tilde{n}})$, Angle of Arrival (AoA) $(\varphi_{\tilde{n}}, \vartheta_{\tilde{n}})$, delay and power characterize the $\tilde{n}$-th cluster and their distributions depend on the considered scenario. Each cluster consists of $\tilde{M}$ unresolvable subpaths and are characterized by the spatial angles $(\phi_{\tilde{n},\tilde{m}}, \theta_{\tilde{n},\tilde{m}})$, $(\varphi_{\tilde{n},\tilde{m}}, \vartheta_{\tilde{n},\tilde{m}})$, $\tilde{m} = 1, \ldots, \tilde{M}_{\tilde{n}}$ as illustrated in Figure 1. Using these definitions, according to 3GPP channel model the channel corresponding to $\tilde{n}$-th cluster for Nonline of Sight (NLOS) case can be modeled as

$$\begin{aligned}(\mathbf{h}_\mathbf{k}^\mathbf{b})^{\tilde{\mathbf{n}}}(\mathbf{t}) = &\sqrt{10^{(-PL+\sigma_{SF})/10}}\sqrt{P_{\tilde{n}}/\tilde{M}_{\tilde{n}}} \\ &\times \sum_{\tilde{m}=1}^{\tilde{M}_{\tilde{n}}}\mathbf{g}_r(\varphi_{\tilde{n},\tilde{m}}, \vartheta_{\tilde{n},\tilde{m}})^T \times \alpha_{\tilde{n},\tilde{m}}\mathbf{g}_t(\phi_{\tilde{n},\tilde{m}}, \theta_{\tilde{n},\tilde{m}}) \\ &\times [\mathbf{a}_r(\varphi_{\tilde{n},\tilde{m}}, \vartheta_{\tilde{n},\tilde{m}})]_l[\mathbf{a}_t(\phi_{\tilde{n},\tilde{m}}, \theta_{\tilde{n},\tilde{m}})]_k \\ &\times exp(i2\pi\upsilon_{\tilde{n},\tilde{m}}t) \end{aligned} \quad (2)$$

where $P_{\tilde{n}}$ is the $\tilde{n}$-th cluster's power, $\upsilon_{\tilde{n},\tilde{m}}$ is the Doppler frequency component that corresponds to $\tilde{m}$-th subpath in $\tilde{n}$-th cluster, PL and σ_{SF} denote the path loss and shadow

fading respectively, $\alpha_{\tilde{n},\tilde{m}}$ describes the coupling between horizontal and vertical polarization for $\tilde{m}$-th subpath in $\tilde{n}$-th cluster, $\mathbf{g}_r(\varphi_{\tilde{n},\tilde{m}}, \vartheta_{\tilde{n},\tilde{m}})$ and $\mathbf{g}_t(\phi_{\tilde{n},\tilde{m}}, \theta_{\tilde{n},\tilde{m}})$ are the radiation patterns of receive and transmit antennas respectively, $\mathbf{a}_r(\varphi_{\tilde{n},\tilde{m}}, \vartheta_{\tilde{n},\tilde{m}})$ and $\mathbf{a}_t(\phi_{\tilde{n},\tilde{m}}, \theta_{\tilde{n},\tilde{m}})$ are the array responses of the transmit and receive antennas respectively. For more detailed channal model analysis, the readers are encouraged to refer to 3GPP's corresponding technical report in [42] and the tutorial paper on full dimensional MIMO architectures of 5G systems in [41].

A. MASSIVE MIMO IMPLEMENTATIONS

Massive MIMO is a refined form of MU MIMO. One of the main differences is that the channel (both in time and frequency) varies more slowly in massive MIMO compared to MU MIMO which brings huge advantages in terms of resource allocation purposes due to better planning. Moreover, for CSI acquisition, massive MIMO mostly depends on UL pilots whereas MU MIMO exploits codebooks. Compared to MU MIMO, massive MIMO has M antennas serving to K_b UEs where typically $M \gg K_b$. Each antenna consists of their own Radio Frequency (RF) and digital baseband chain. The tight phase control is maintained by BSs to process the signals from all antennas. In practice, massive MIMO dynamically switches between SU and MU MIMO depending on network conditions and the application requirements while modifying the shape and length of the beam at the same time. Both massive and MU MIMO aim to increase the UE data throughput and system capacity to meet the requirements defined in 5G standards. They leverage massive MIMO to dynamically transmit data streams as highly-focused beams and exploit multi-path propagation and spatial multiplexing to transmit and receive multiple data streams simultaneously over the same radio channel. Hence together with beam steering, a stronger radio signal yielding high throughput can be achieved for each UE in the network.

Fig. 2 shows the comparisons of two different MIMO implementations for SU-MIMO and MU massive MIMO scenarios. In SU-MIMO scenario of Fig. 2(a), multiple data streams are sent to a SU using multiple antennas under the same spectrum and time resources. This allows UEs to send and receive data streams simultaneously while increasing the user peak throughput (that is usually limited by the number of antennas at UE). Massive MIMO with MUs in Fig. 2(b) on the other hand, further increases the cell throughput and the overall performance, thanks to spatial multiplexing between different UEs. Together with MU beamforming, multiple UEs can be enabled to utilize the same time and frequency resources simultaneously. Hence, data is streamed to many UEs in MU massive MIMO implementation. It can also support high number of layers (e.g. up to 16 layers).

B. TDD-BASED MASSIVE MIMO

One consideration that needs to be taken into account is the utilization of TDD or FDD in 5G networks. They both provide paths to UL and DL traffic. However, some substantial

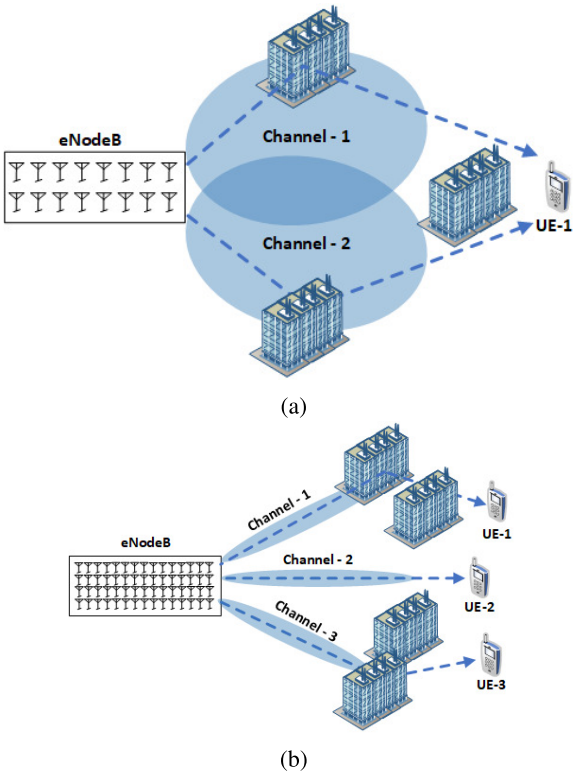

FIGURE 2. Comparisons of different MIMO implementations (a) SU MIMO (b) Massive MIMO with MUs.

differences between them exist when they are used within the context of massive MIMO. Due to existence of pilot overhead and CSI feedback requirement in FDD operation [43], massive MIMO works better in TDD systems in terms of deployment flexibility and efficient spectrum utilization.

TDD relies on channel reciprocity and only requires orthogonal pilots in the UL from K UEs. Depending on several conditions such as traffic load, pattern and user distribution, TDD-based massive MIMO can bring several benefits for MNOs. It can allow increased number of antennas and exploit channel reciprocity. Due to small variations on link quality, better resource allocation can be performed [43]. As a result, TDD is a better choice for massive MIMO systems in terms of avoiding the complexity associated with channel estimation and channel sharing when compared with FDD. For these reasons, our experimental results focus on TDD implementation of massive MIMO.

Table 1 shows the comparisons of multi antenna transmission modes: SU and MU MIMO FDD, Massive MIMO FDD and TDD strategies to provide MNO services for cellular networks. During our tests, we have experimented SU MIMO FDD (named as FDD-based MIMO) and massive MIMO TDD (named as TDD-based massive MIMO).

IV. EXPERIMENTAL EVALUATIONS

The main aim of the experimental setup is to test and observe the massive MIMO solution in a real world operating

TABLE 1. Comparisons of multi antenna transmission modes: single user (SU), multi user (MU) and massive MIMO FDD and massive MIMO TDD strategies.

MIMO Strategy	Characteristics	Challenges	Advantages
Single-User MIMO FDD	— BS radiates one signal uniformly — An example of SDM (Spatial Division Multiplexing). — Precoding give rise different patterns to antennas. — Exploit the multi path propagation geometry in two different ways as the UE moves.	— Must find a precoder matrix that gives orthogonal streams. — The receiver must perform antenna demapping. — Apply the receiver precoder on its receiver antenna ports.	— If the UE moves a different precoder will be used — Mature technology with low practical constraints. — Increases the data rate by creating several layers when less users exist. — Benefits regardless of load.
Multi-User MIMO FDD	— BS radiates multiple signals focused on UEs — Small number of BS antennas (M ∼2-8) serving to users, (K_b ∼1-4) in general $K_b \sim M$. — CSI acquisition is based on predefined codebooks with specific angular beams. — Spatially multiplexed UEs allocated to same resource blocks.	— Channel quality varies due to freq. selective channel and small-scale fading. — Resource allocations change fast due to high channel variations. — Ineffective interference suppression due to small number of antennas — Each UE does not experience a data rate multiplication as with SU-MIMO.	— Several UEs can communicate with BS using the same resources. — Ideally M (# of antennas) times signal strength compared to SU MIMO. — Small pilot overhead. — The cell benefits from the reuse of the resources.
Massive MIMO FDD	— Refined form of MU MIMO FDD. — Hundreds of BS antennas (∼100 to ∼1000), serving multiple users (∼16 to ∼64). — High spatial resolution.	— Requires significant pilot & feedback overhead for CSI acquisition. — Channel reciprocity cannot be exploited. — CRS not used but needs to be present for legacy UEs (additional overhead for TM9 UEs) — High RS density required for demodulation.	— Continuous traffic results low latency. — Robustness against interference. — Backward compatibility (since FDD is commonly deployed). — Improve spectrum and energy efficiency by orders of magnitude. — Channel quality varies slowly over space & time with channel hardening. — Better resource allocation&planning due to slow varying channel.
Massive MIMO TDD	— Massive MIMO initially designed in TDD mode due to channel reciprocity. — Hundreds of BS antennas (∼100 to ∼1000), serving multiple users (∼16 to ∼64). — CSI acquisition is based on uplink pilot transmission and channel reciprocity. — High spatial resolution.	— Interference between time slots (due to synchronization issues.) — Inter-cell interference caused by pilot contamination. — Can enter saturation i.e. additional BS antennas do not increase throughput. — Received CSI at the transmitter can be outdated. — Coherence interval constraint. — Power consumption.	— Channel reciprocity. — Frequency diversity is larger. — Allows unpaired band allocations. — Channel quality varies slowly over space and time thanks to channel hardening. — Better resource allocation and planning due to slow varying channel.

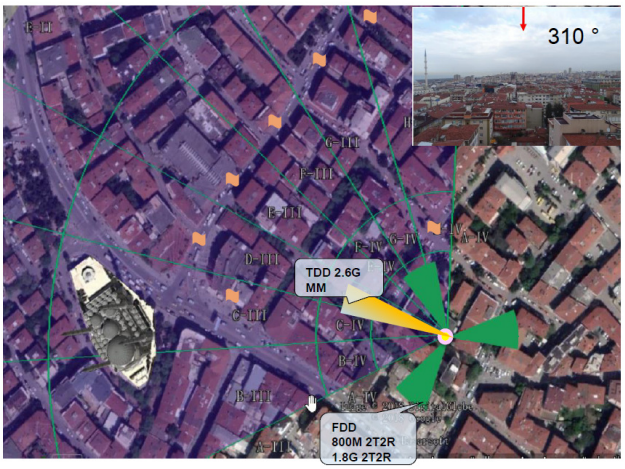

FIGURE 3. Location and azimuth angles of the experimental massive MIMO test environment.

environment of a telecommunication operator. Fig. 3 shows the location and azimuth angles of the prepared test environment in Istanbul, Turkey where $L = 1$ cell is equipped with massive MIMO having $M = 64$ antennas. Our experiments for monitoring and comparisons of both TDD-based massive MIMO and FDD-based MIMO deployments were performed between 16−18 September 2018 and 23−25 September 2018 respectively. Each measurements are collected and averaged over one hour intervals. TDD-based massive MIMO operates @2.6 GHz with $64T64R$ on areas pointed with yellow beams and co-site FDD-based MIMO operates @800 MHz and @1.8 GHZ with $2T2R$ on areas pointed with green colored

TABLE 2. Experimental network parameters.

Parameter	Value	Parameter	Value
Carrier Frequency	2575 - 2615 MHz (2.6GHz B38)	Receiver noise power	-112 dBm
Number of subcarriers	600	Subcarrier bandwidth	15 kHz
Cyclic prefix overhead	6.67%	Frame dimensions	10 ms
Tx Power	120W	Occupied Bandwidth	10 Mhz
Antenna	64T64R	Transmission Scheme	OFDM

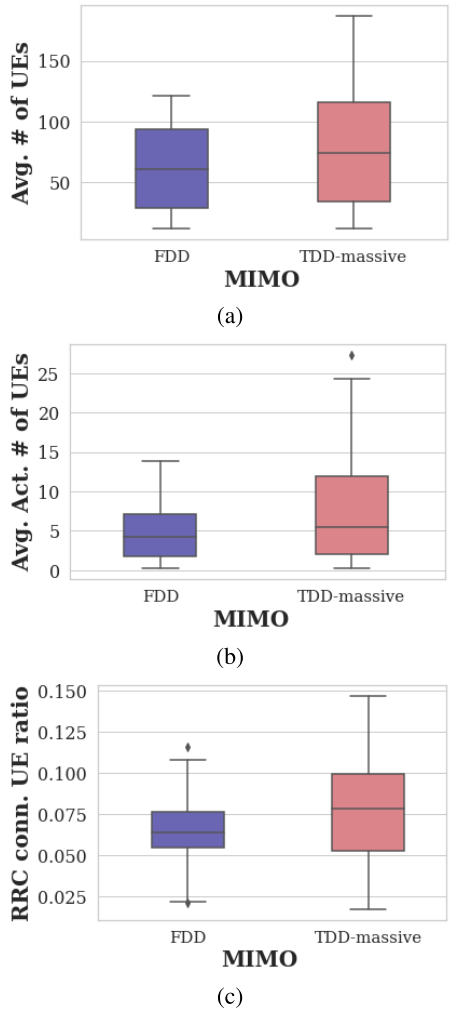

FIGURE 4. Boxplot comparisons for different number of UEs for FDD-bsed MIMO and TDD-based massive MIMO (a) Average number of UEs (b) Average number of active UEs (c) RRC connected user ratio.

beams in Fig. 3. Table 2 shows the experimental parameters and their corresponding values used throughout TDD-based massive MIMO experiments. In the rest of the paper, unless otherwise stated TDD-based massive MIMO operates at 10 Mhz bandwidth and FDD-based MIMO operates at 20 Mhz bandwidth under the same site when different KPIs are compared. During the experimental tests, Transmission Mode (TM)9 capable UEs of LTE Release 10 are used.

A. RESULT ANALYSIS

Comparison of User Numbers: Fig. 4 shows the boxplot comparisons for different number of UEs (K) when TDD-based massive MIMO and FDD-based MIMO are utilized. The RRC connected ratio in Fig. 4c is simply calculated as ratio between the average active user and average user. First of all, from all the sub-graphs, we can observe that average number of UEs, average number of active UEs and RRC connected UE ratios have increased after TDD-based massive MIMO is activated. Hence, we can infer that together with the increase

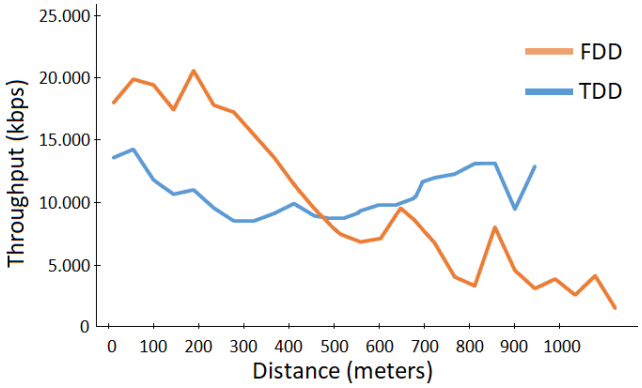

FIGURE 5. DL throughput performance comparisons of FDD at 20 Mhz bandwidth and TDD-based massive MIMO deployments at 10 Mhz bandwidth versus increasing distance between UE and BS in operational mobile network.

in the number of average active UEs, higher signal strength and coverage are achieved for all UEs during the observation period. UEs that are served under TDD-based massive MIMO, especially on the cell edge, are now connected to the eNodeB as active UEs. Hence, UEs that were previously in cell edge are now included in cell's coverage.

FDD-Based MIMO vs. TDD-Based Massive MIMO Implementations: Fig. 5 shows performance comparisons of FDD-based MIMO at 20 Mhz and TDD-based massive MIMO at 10 Mhz implementation's DL throughput values versus the increasing distance in our real experimental mobile network implementation for two different test UEs. Table 3 on the other hand, shows the corresponding Reference Signal Received Power (RSRP), signal-to-interference-plus-noise ratio (SINR) and application layer throughput measurement values for the near, mid and far test point locations of one of test UE for TDD-based massive MIMO. We can observe from Table 3 that good application layer throughput values are achieved in mid-to-far point of the BS with TDD-based massive MIMO. In fact, massive MIMO enables a phenomenon called "channel hardening" which effectively eliminates multi-path fading yielding relatively good SINR and DL throughput values in mid/far regions. However, path loss is still dominant for UEs that are located far from the BSs. This is also observed with average RSRP values of Table 3 where far site UEs can experience up to 26 dB loss compared to near site UEs.

TABLE 3. RSRP, SINR and application layer throughput for different test locations.

Test Point	RSRP (Avg)	SINR(Avg)	Application Layer DL Throughput (kbps)
Near	-76.88	23.44	13304.92
Mid	-84.66	23.37	11224.23
Far	-102.65	23.3	10353.12

From Fig. 5, we can also observe the existence of a trade-off between FDD-based MIMO and TDD-based

massive MIMO deployments. It is known that FDD can cover larger areas whereas TDD can provide higher capacity. We can observe from Fig. 5 that at low distances between the BS and UE, FDD-based MIMO with 20 Mhz performs better than TDD-based massive MIMO with 10 Mhz bandwidth until a distance of 500 metres since FDD's bandwidth is also higher than TDD. However as the distance increases, the advantage of TDD-based massive MIMO supersedes over FDD-based MIMO. Hence from Fig. 5, the throughput of FDD degrades significantly whereas the throughput of TDD is observed to be more robust especially in mid/far distance due to exploitation of massive MIMO. Hence, massive MIMO has provided consistent service to all UEs over the coverage area.

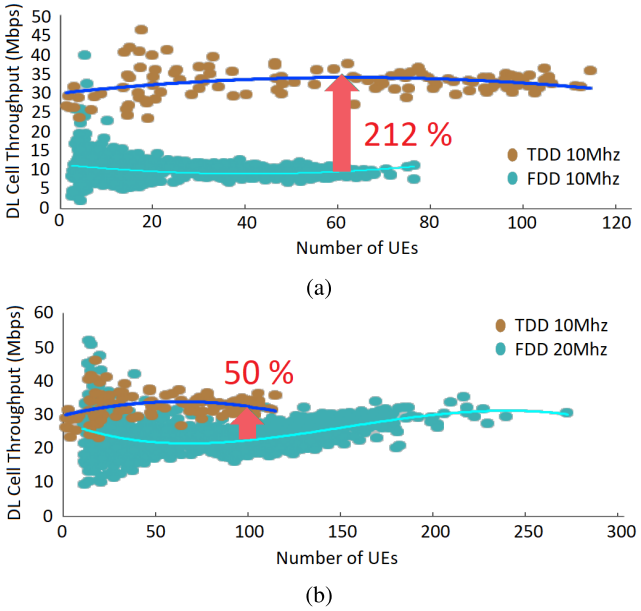

FIGURE 6. Scatter plot for experimental test result comparisons for increasing number of UEs (K) for scenarios: (a) FDD-based MIMO with 10 Mhz bandwidth v.s. TDD-based massive MIMO with 10 Mhz bandwidth. (b) FDD-based MIMO with 20 Mhz bandwidth v.s. TDD-based massive MIMO with 10 Mhz bandwidth.

Fig. 6 shows the scatter plot for MIMO experimental test result comparisons of DL cell throughput during busy hour traffic versus the increasing number of UEs based on co-sites commercial user traffic. In both Fig. 6a and Fig. 6b, blue colored line represents the fitted regression line for TDD-based massive MIMO case whereas cyan colored line represents the fitted regression line for FDD-based MIMO case. Fig. 6a shows the comparisons for case of FDD-based MIMO and TDD-based massive MIMO both in 10 Mhz bandwidth. The number of UEs in TDD case has exceeded up to 120 UEs whereas it has gone up to 80 UEs in FDD scenario. We can observe from Fig. 6a that TDD-based massive MIMO with 10 Mhz bandwidth yields approximately 212% improvements when number of UEs is around $K = 60$ compared to FDD-based MIMO in 10 Mhz bandwidth. This shows the clear advantage of TDD-based massive MIMO compared to FDD-based MIMO under same bandwidth. Fig. 6b shows the comparisons for the case of FDD-based MIMO with 20 Mhz bandwidth and TDD-based massive MIMO in 10 Mhz bandwidth. In this case, due to higher bandwidth utilization of FDD systems, higher DL cell throughput values are obtained. However, TDD-based massive MIMO still performs better than FDD-based MIMO. For example, when the number of UEs is $K = 100$, the improvement is approximately 50%. One of the other reason for this improvement is that using TM9 devices in the experiments has made it possible to use both SU MIMO and massive MIMO transmission modes. Additionally, the TDD system used in the test has the capability of dynamic switching between TM9 and TM4 which supports closed loop spatial multiplexing. This has facilitated dynamic switching between both modes without special signaling by higher layers.

Fig. 7 provides the average Physical Resource Block (PRB) utilization percentages measured at each layers with TDD-based massive MIMO. In Fig. 7, the most PRB utilization are concentrated at first three layers. Out of all available PRB, the first layer has 53.5% followed by layer 2 with 29.95% and third layer with 15.53%. Most of the time only first three layers are observed which can be due to low pairing opportunities as a consequence of the UE traffic that is bursty and with low payload profile. Thus based on low number of layer selections, we can conclude that few pairing occasions per TTI have occurred.

Fig. 8 gives some of the monitored KPIs before and after the experimental massive MIMO tests between $16-18$ September 2018 (when FDD-based MIMO is ON) and $23-25$ September 2018 (when TDD-based massive MIMO is activated) all in hourly intervals. In all the observed time-series plots of Fig. 8, a similar trend exists where all KPI values are always at low base at night and high peak at daytime. Fig. 8a shows the results for changes in average number of total users in the experimental site over the observation duration. Before activation of TDD-based massive MIMO in FDD-based MIMO, there are $K = 65$ UEs inside the cell whereas after activation the number of UEs increases to $K = 80$ on average. However, not all UEs are active inside the cell during our observation duration. Fig. 8b shows the variation of active number of UEs. Average number of active UEs has increased from 4 to 8 after TDD-based massive MIMO activation. Finally, Fig. 8c shows the change in total volume of PS traffic. We can observe from Fig. 8c that the average of total volume of PS traffic has also increased during TDD-based massive MIMO tests. The average traffic is on the order of 5.8 GB in TDD-based massive MIMO whereas it is around 4.3 GB in FDD-based MIMO.

The efficient suppression of interference together with TDD-based beamforming has extended cell-edge coverage, i.e. for UEs that have poor SINR before TDD-based massive MIMO activation. Multiple antennas allow to receive beamforming with certain direction of arrival. However, beamforming also requires accurate channel estimation of UEs. The complexity and type of MIMO in 3GPP is defined

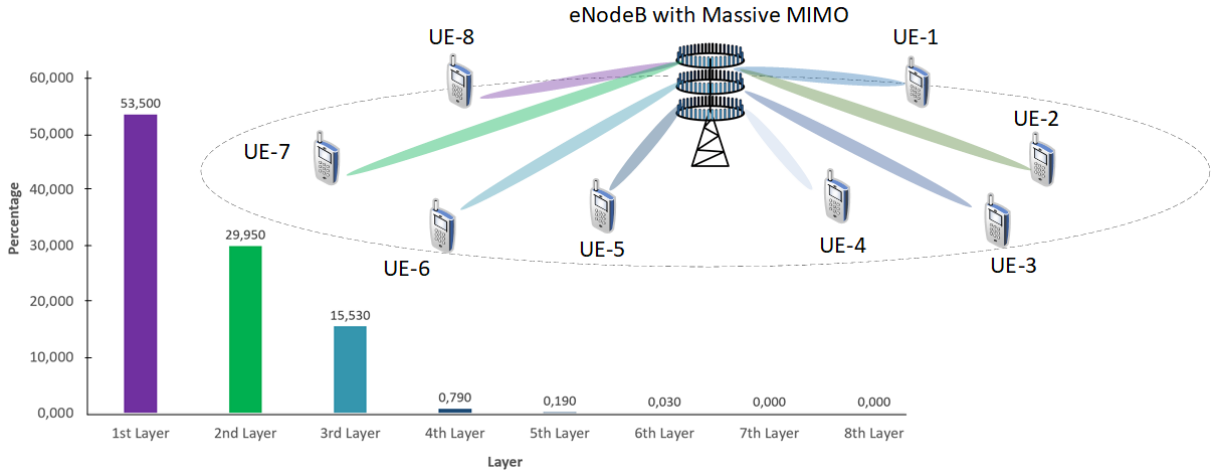

FIGURE 7. Average PRB utilization percentages measured at each layer with TDD-based massive MIMO.

using TMs [44]. The difference arises between TMs based on number of layers, utilized antenna ports, precoding types or type of Reference Signal (RS), Cell-specific Reference Signal (CRS) or Demodulation Reference Signals (DMRS). The utilization of TM9 capable UEs in TDD-based massive MIMO is shown to exhibit the most benefit in cell edge conditions since beamforming has improved the quality of UE's received signal. TM9-capable UEs that are used for experiments allow BSs to build user dedicated beams towards UE and also includes more accurate CSI measurements. Different methods of channel estimation are available for TDD and FDD LTE systems. The transmission modes used for beamforming in TM9 utilize additional RSs to help with demodulation and determine CSI. These additional RSs help to reduce the number of resource elements that are available for the Physical Downlink Shared Channel (PDSCH). As a matter of fact, TM9 uses an enhanced reference signal structure and has the following types of reference signals: UE-specific DMRS for demodulation of PDSCH and CSI-RS for UE DL CSI measurements. For these reasons, the accuracy of CSI reports are also higher than other TMs such as TM8.

Fig. 9 shows the boxplot comparisons of different KPIs for both FDD-based MIMO and TDD-based massive MIMO in the considered commercial site. Fig. 9a shows the cell throughput values which are the total PS values in both UL and DL whereas Fig. 9b shows the DL PS traffic volume. Cell throughput measures the cell capacity. From Fig. 9a, we can observe that activating TDD-based massive MIMO has increased the median traffic volume from 4.63 to 6.32 (i.e. 36% increase) for all PS traffic and from Fig. 9b, TDD-based massive MIMO has increased the DL PS traffic from 4.21 to 5.80 (i.e. 38% increase). However, realized amount of traffic increase is below expectations. One major reason for relatively low increase of 36% in total PS volume after TDD-based massive MIMO activation is the utilization of higher bandwidth in FDD-based MIMO (20 Mhz compared to 10 Mhz). Another reason can be due to the location of the UEs, non-uniform horizontal distribution of UEs with Line of Sight (LOS) inside the coverage area as well as the inclusion of high number of UEs with NLOS in TDD-based massive MIMO integration. Non-uniform horizontal UE distribution implies that the UEs are positioned in close proximity to each other within the coverage area. The gain ratios may also vary according to whether the UEs are in different TMs [45].

Fig. 9c shows the UL SE values. The SE measures simply the bits per PRB in Hz. It is calculated as UL cell throughput in bits divided by number of PRBs used by Physical Uplink Shared Channel (PUSCH) dedicated radio bearer per msec, Resource Block (RB) in Hz and number of UL antennas. From Fig. 9c, the median UL SE value has increased from 266.78 bps/Hz to 290.76 bps/Hz (i.e. 9% increase) when TDD-based massive MIMO feature is activated. Fig. 9d shows the DL schedule TTI duty cycle percentage values. DL schedule TTI duty cycle percentage simply measures the number of times that UEs are scheduled in a cell in the DL direction per msec, RB and number of DL antennas. Together with activation of TDD-based massive MIMO with 10 Mhz bandwidth, median value of the duty cycle percentage has increased from 0.69 to 0.79 (i.e. 14.5% increase) in comparison to FDD-based MIMO with 20 Mhz bandwidth. The increase in TTI duty cycle indicates the utilization opportunities provided by TDD-based massive MIMO where UEs are co-scheduled on TTI basis. Moreover, continuous data transmission (e.g. file downloading or video streaming) also brings high data demand for active user per TTI where massive MIMO can provide enhanced opportunities.

Fig. 10 shows the comparisons of paired layers in DL versus the number of active users for TDD-based massive MIMO. The average DL paired layer is observed to be 2.43 and in busy hour it can reach to up to 4 paired layers with 120 RRC connect user. Therefore, we can observe that in TDD-based massive MIMO deployment scenario, there

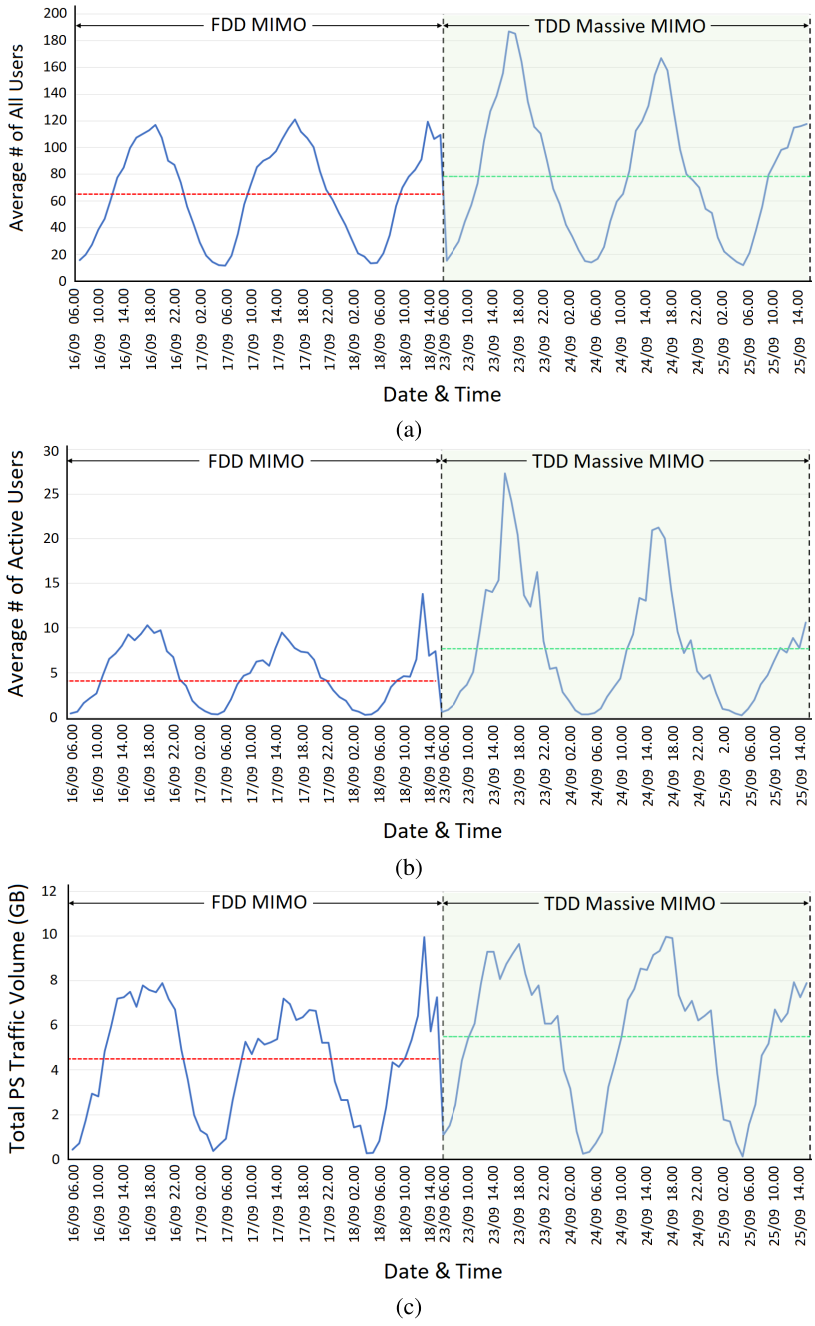

FIGURE 8. Different observed KPIs for TDD-based massive MIMO and FDD-based MIMO. (a) Average number of total UEs. (b) Average number of active UEs. (c) Total volume of PS traffic.

is still a room for cell throughput enhancements with more active users. Furthermore, if UEs are stationary it can be assumed that the channel/spatial isolation wouldn't be changing with time. In that case, a relationship between UE distribution and traffic pattern can also be inferred. If the UEs are spatially separated but in a mobile state, then it is possible that at some instance they can get closer to each other. In that case, since the large packet sizes provides more time to pairing opportunity, the gains may be further increased due to availability of more time to pair UEs in comparison with small sized packets in mobility conditions.

B. DISCUSSION

The number of RRC connected UEs and the cell throughput have a direct effect on the performance of UEs using massive MIMO. Normally as the number of RRC connected UEs increases, the pairing opportunities between UEs are expected to increase. However, the SRS resources are limited

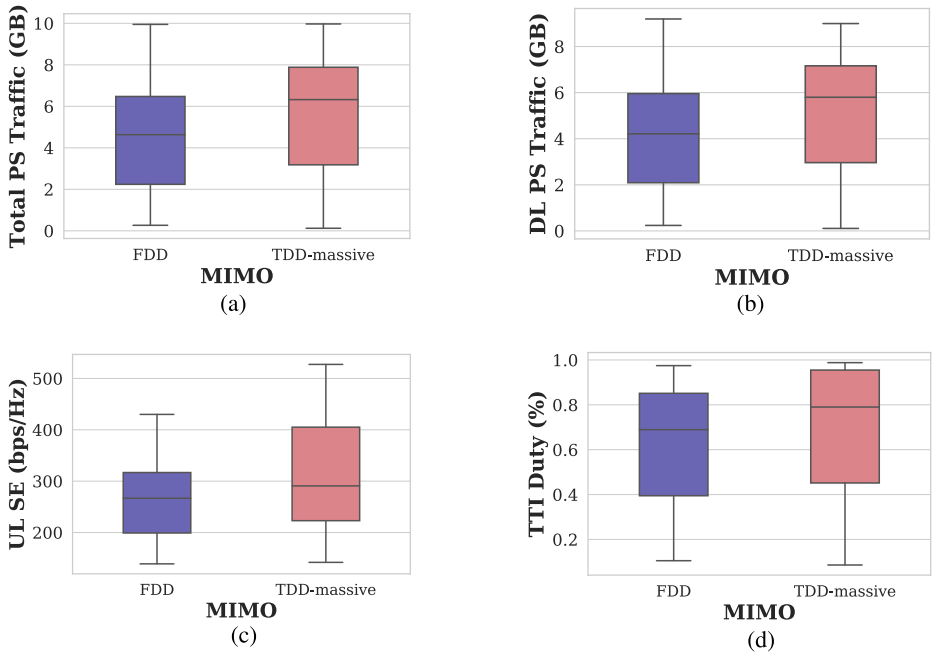

FIGURE 9. Boxplot comparisons for different KPIs for FDD-based MIMO and TDD-based massive MIMO. (a) Total PS traffic (UL and DL). (b) DL PS traffic. (c) UL spectral efficiency. (d) DL schedule TTI duty cycle percentage.

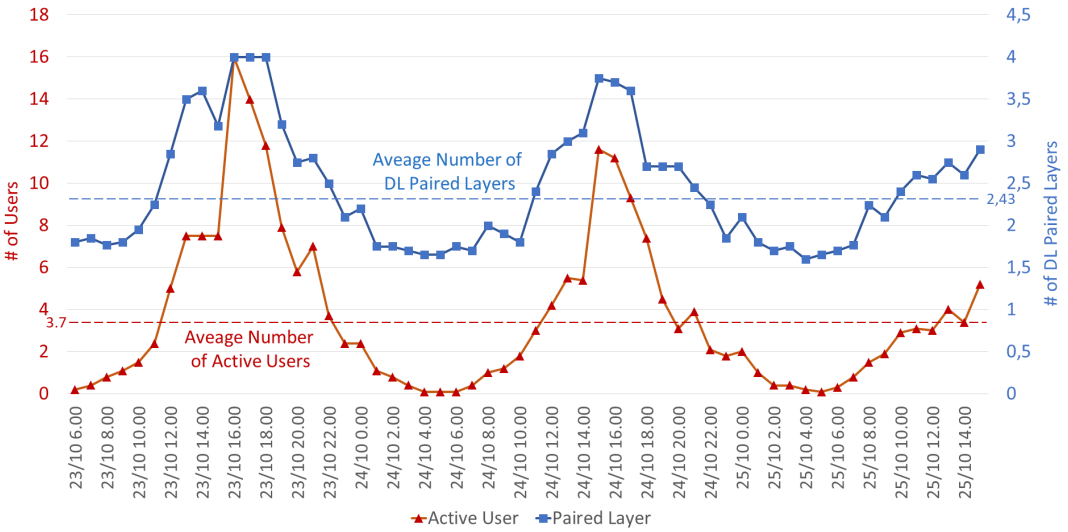

FIGURE 10. Comparisons of paired layers in DL vs. number of active users in TDD-based massive MIMO.

per cell as well. For example, for a SRS resource of 128 per BS that has 3 cell configuration, one cell will have 64 of resources and each of the other two will have 32 SRS resources. In this case, more RRC connected UEs above the available number of SRS resources will decrease the pairing opportunities, as the UEs to be scheduled in a given TTI will be a mix of TDD-based massive MIMO user and FDD-based SU candidates. This fact reveals a trade-off between the high number of RRC connected UEs and available number of SRS resources. Therefore, although the pairing opportunities between the UEs is expected to increase with massive MIMO design, limited SRS resources will have detrimental affect on the advantages proposed by massive MIMO. During our experimental tests, the number of RRC connected UEs is observed to be low (on average of 6). Due to low number of RRC connected UEs, SRS limitations are not considered to have big impact on pairing opportunities and the performance of massive MIMO deployments.

In addition to above, the amount of PRB usage for every scheduling occasion determines the number of TDD-based

MU candidates that will be scheduled in a given TTI cycle. If the cell throughput becomes low, then UEs will be handled as SU candidates, otherwise they will be handled as MU candidates by the massive MIMO deployment system. Therefore, more data to transmit has a direct impact on the number of scheduling occasions. In that case, UEs will need to empty their buffer which increases the pairing opportunities over time.

V. CONCLUSION AND FUTURE WORK

Massive MIMO is expected to bring major advantages to MNOs to meet the stringent requirements of 5G. This paper has presented a real-world deployment analysis of massive MIMO in a commercial network environment based in Turkey. In particular, various KPIs have been monitored and comparisons are made between TDD-based massive MIMO and FDD-based MIMO deployments. The experiments results revealed that TDD-based massive MIMO in 10 Mhz bandwidth reveals up to 212% and 50% higher cell throughput than FDD-based MIMO in 10 and 20 Mhz bandwidth respectively. The DL throughput is also observed to be better in mid/far points for TDD-based massive MIMO when FDD-based MIMO in 20 Mhz bandwidth is compared with TDD-based massive MIMO in 10 Mhz bandwidth. Our experimental results also indicated that in TDD-based massive MIMO, median values of total cell PS traffic, UL SE and DL schedule TTI duty cycle can be improved by 38%, 9% and 14.5% respectively compared to FDD-based MIMO scenario. At the end of the paper, we have also discussed about possible trade-offs in terms of RRC-connected UEs, cell throughput, available SRS resources and pairing opportunities that can be encountered in future massive MIMO deployments. As a future work, a dynamic method that makes scheduling decisions at every scheduling interval based on the status of channel based on measurements, co-channel interference and data traffic modeling behaviour can be evaluated so that the UEs will be appropriately handled in SU, MU or massive MIMO scenarios.

REFERENCES

[1] I. Selinis, K. Katsaros, M. Allayioti, S. Vahid, and R. Tafazolli, "The race to 5G era; LTE and Wi-Fi," *IEEE Access*, vol. 6, pp. 56598–56636, 2018.

[2] M. Maternia. (2016). *5G PPP Use Cases and Performance Evaluation Models*. Accessed: Jul. 21, 2019. [Online]. Available: https://bit.ly/30NZQzo

[3] M. Agiwal, A. Roy, and N. Saxena, "Next generation 5G wireless networks: A comprehensive survey," *IEEE Commun. Surveys Tuts.*, vol. 18, no. 3, pp. 1617–1655, Feb. 2016.

[4] D. C. Araújo, T. Maksymyuk, A. L. F. de Almeida, T. Maciel, J. C. M. Mota, and M. Jo, "Massive MIMO: Survey and future research topics," *IET Commun.*, vol. 10, no. 15, pp. 1938–1946, Oct. 2016.

[5] S. Buzzi, C.-L. I, T. E. Klein, H. V. Poor, C. Yang, and A. Zappone, "A survey of energy-efficient techniques for 5G networks and challenges ahead," *IEEE J. Sel. Areas Commun.*, vol. 34, no. 4, pp. 697–709, Apr. 2016.

[6] Amy Nordrum. (2016). *5G Researchers Set New World Record for Spectrum Efficiency*. Accessed: May 28, 2019. [Online]. Available: https://bit.ly/2LdO5KA

[7] GSMA. (2019). *5G Implementation Guidelines*. Accessed: Jul. 21, 2019. [Online]. Available: https://bit.ly/2O92gao

[8] E. G. Larsson and L. Van der Perre, "Massive MIMO for 5G," *IEEE 5G Tech Focus*, vol. 1, no. 1, pp. 1–4, Mar. 2017.

[9] D. Schoolar, "Massive MIMO comes of age," Samsung Electron., Ovium, London, U.K., White Paper 1, 2017. Accessed: Feb. 15, 2020. [Online]. Available: https://bit.ly/2u12es5

[10] E. Björnson, L. Sanguinetti, H. Wymeersch, J. Hoydis, and T. L. Marzetta, "Massive MIMO is a reality—What is next?: Five promising research directions for antenna arrays," *Digit. Signal Process.*, vol. 94, pp. 3–20, Nov. 2019.

[11] Huawei Technologies Company, Ltd. (2018). *Active Antenna Unit (AAU)*. Accessed: May 28, 2019. [Online]. Available: https://bit.ly/2K7SKkp

[12] Ericsson. (2018). *Antenna Integrated Radio Unit Description AIR 6468*. Accessed: May 28, 2019. [Online]. Available: https://bit.ly/2JHEaRl

[13] Nokia. (2018). *AirScale Base Station*. Accessed: May 28, 2019. [Online]. Available: https://nokia.ly/2HYa3le

[14] L. Sanguinetti, E. Björnson, and J. Hoydis, "Towards massive MIMO 2.0: Understanding spatial correlation, interference suppression, and pilot contamination," 2019, *arXiv:1904.03406*. [Online]. Available: http://arxiv.org/abs/1904.03406

[15] C. Bouras, S. Kokkalis, A. Kollia, and A. Papazois, "Techno-economic comparison of MIMO and DAS cost models in 5G networks," *Wireless Netw.*, vol. 26, no. 1, pp. 1–15, Jan. 2020.

[16] Sprint. (2018). *Sprint Unveils Six 5G-Ready Cities*. Accessed: May 28, 2018. [Online]. Available: https://sprint.co/2ED4YOv

[17] Mike Hennigan. (2018). *Sprint is Getting Ready for the Big Game and 5G in Atlanta*. Accessed: May 28, 2019. [Online]. Available: https://sprint.co/2Qc3x1f

[18] Verizon. (2018). *Verizon Trial for Massive MIMO Advancements, on the Path to 5G*. Accessed: Dec. 17, 2018. [Online]. Available: https://goo.gl/d3PGuL

[19] O2 UK. (2018). *O2's 5G-Focused Massive MIMO Trial in London*. Accessed: Dec. 17, 2018. [Online]. Available: https://goo.gl/kJaduK

[20] Emil Björnson. (2019). *Increasing the Spectral Efficiency of FutureWireless Networks*. Accessed: Jul. 21, 2019. [Online]. Available: https://bit.ly/2YkZ4wg

[21] (2019). *How Much Does Massive MIMO Improve the Spectral Efficiency*. Accessed: Jul. 21, 2019. [Online]. Available: https://bit.ly/2GovWtX

[22] J. Flordelis, F. Rusek, F. Tufvesson, E. G. Larsson, and O. Edfors, "Massive MIMO performance—TDD versus FDD: What do measurements say?" *IEEE Trans. Wireless Commun.*, vol. 17, no. 4, pp. 2247–2261, Apr. 2018.

[23] S. Malkowsky, J. Vieira, L. Liu, P. Harris, K. Nieman, N. Kundargi, I. C. Wong, F. Tufvesson, V. Owall, and O. Edfors, "The world's first real-time testbed for massive MIMO: Design, implementation, and validation," *IEEE Access*, vol. 5, pp. 9073–9088, 2017.

[24] W. Zhang, J. Xiang, Y.-N.-R. Li, Y. Wang, Y. Chen, P. Geng, and Z. Lu, "Field trial and future enhancements for TDD massive MIMO networks," in *Proc. IEEE 26th Annu. Int. Symp. Pers., Indoor, Mobile Radio Commun. (PIMRC)*, Aug. 2015, pp. 2339–2343.

[25] X. Gao, O. Edfors, F. Rusek, and F. Tufvesson, "Massive MIMO performance evaluation based on measured propagation data," *IEEE Trans. Wireless Commun.*, vol. 14, no. 7, pp. 3899–3911, 2015.

[26] X. Wang, "Large scale experimental trial of 5G mobile communication systems—TDD massive MIMO with linear and non-linear precoding schemes," in *Proc. IEEE 27th Annu. Int. Symp. Pers., Indoor, Mobile Radio Commun. (PIMRC)*, Sep. 2016, pp. 1–5.

[27] A. Yang, C. Xing, Z. Fei, and J. Kuang, "Performance analysis for uplink massive MIMO systems with a large and random number of UEs," *Sci. China Inf. Sci.*, vol. 59, no. 2, pp. 1–9, Feb. 2016.

[28] W. Wang, W. Liang, B. Li, L. Gu, J. Sheng, P. Qiu, J. Wang, and Y. Wang, "Field trial on TDD massive MIMO system with polar code," in *Proc. IEEE 28th Annu. Int. Symp. Pers., Indoor, Mobile Radio Commun. (PIMRC)*, Oct. 2017, pp. 1–6.

[29] X. Yang, W. Lu, N. Wang, K. Nieman, C.-K. Wen, C. Zhang, S. Jin, X. Mu, I. Wong, Y. Huang, and X. You, "Design and implementation of a TDD-based 128-antenna massive MIMO prototype system," *China Commun.*, vol. 14, no. 12, pp. 162–187, Dec. 2017.

[30] M. Alkhaled, E. Alsusa, and D. K. C. So, "On the performance of TDD massive MIMO systems with pilot contamination," in *Proc. IEEE 85th Veh. Technol. Conf. (VTC Spring)*, Jun. 2017, pp. 1–6.

[31] X. Jiang, F. Kaltenberger, and L. Deneire, "How accurately should we calibrate a massive MIMO TDD system?" in *Proc. IEEE Int. Conf. Commun. Workshops (ICC)*, May 2016, pp. 706–711.

[32] A. Gupta and R. K. Jha, "Power optimization using massive MIMO and small cells approach in different deployment scenarios," *Wireless Netw.*, vol. 23, no. 3, pp. 959–973, Apr. 2017.

[33] J. Hoydis, S. T. Brink, and M. Debbah, "Massive MIMO in the UL/DL of cellular networks: How many antennas do we need?" *IEEE J. Sel. Areas Commun.*, vol. 31, no. 2, pp. 160–171, Feb. 2013.
[34] V. Saxena, G. Fodor, and E. Karipidis, "Mitigating pilot contamination by pilot reuse and power control schemes for massive MIMO systems," in *Proc. IEEE 81st Veh. Technol. Conf. (VTC Spring)*, May 2015, pp. 1–6.
[35] H. Xie, F. Gao, S. Zhang, and S. Jin, "A unified transmission strategy for TDD/FDD massive MIMO systems with spatial basis expansion model," *IEEE Trans. Veh. Technol.*, vol. 66, no. 4, pp. 3170–3184, Apr. 2017.
[36] J. Ma, S. Zhang, H. Li, F. Gao, and S. Jin, "Sparse Bayesian learning for the time-varying massive MIMO channels: Acquisition and tracking," *IEEE Trans. Commun.*, vol. 67, no. 3, pp. 1925–1938, Mar. 2019.
[37] J. Ma, S. Zhang, H. Li, N. Zhao, and V. C. M. Leung, "Interference-alignment and soft-space-reuse based cooperative transmission for multi-cell massive MIMO networks," *IEEE Trans. Wireless Commun.*, vol. 17, no. 3, pp. 1907–1922, Mar. 2018.
[38] A. Adhikary, J. Nam, J.-Y. Ahn, and G. Caire, "Joint spatial division and multiplexing—The large-scale array regime," *IEEE Trans. Inf. Theory*, vol. 59, no. 10, pp. 6441–6463, Jun. 2013.
[39] Z. Jiang, A. F. Molisch, G. Caire, and Z. Niu, "Achievable rates of FDD massive MIMO systems with spatial channel correlation," *IEEE Trans. Wireless Commun.*, vol. 14, no. 5, pp. 2868–2882, May 2015.
[40] J. Vieira, F. Rusek, O. Edfors, S. Malkowsky, L. Liu, and F. Tufvesson, "Reciprocity calibration for massive MIMO: Proposal, modeling, and validation," *IEEE Trans. Wireless Commun.*, vol. 16, no. 5, pp. 3042–3056, May 2017.
[41] Q.-U.-A. Nadeem, A. Kammoun, and M.-S. Alouini, "Elevation beamforming with full dimension MIMO architectures in 5G systems: A tutorial," *IEEE Commun. Surveys Tuts.*, vol. 21, no. 4, pp. 3238–3273, 2019.
[42] *Study on 3D Channel Model for LTE (V12.7.0)*, document TR36.873, 3GPP, 2017.
[43] E. Björnson, E. G. Larsson, and T. L. Marzetta, "Massive MIMO: Ten myths and one critical question," *IEEE Commun. Mag.*, vol. 54, no. 2, pp. 114–123, Feb. 2016.
[44] J. Wannstrom. (2013). *LTE-Advanced*. Accessed: Jan. 12, 2020. [Online]. Available: https://bit.ly/2uEINFq
[45] X. Zhang, X. Gu, W. Li, L. Zhang, J. Shen, and Y. Wan, "The study of indoor and field trials on MIMO architecture in TD-LTE network," *Int. J. Antennas Propag.*, vol. 2013, Apr. 2013, Art. no. 181579.

ENGIN ZEYDAN (Member, IEEE) received the B.Sc. and M.Sc. degrees from the Department of Electrical and Electronics Engineering, Middle East Technical University, Ankara, Turkey, in 2004 and 2006, respectively, and the Ph.D. degree from the Department of Electrical and Computer Engineering, Stevens Institute of Technology, Hoboken, NJ, USA, in February 2011. He has worked as an R&D Engineer of Avea, a mobile operator in Turkey, from 2011 to 2016. He was with Türk Telekom Labs working as a Senior R&D Engineer, from 2016 to 2018. He was also part-time Instructor with the Electrical and Electronics Engineering Department, Ozyegin University, from 2015 to 2018. He is currently working as a Researcher with the Communication Networks Division, Centre Tecnologic de Telecomunicacions de Catalunya (CTTC). His research interests are in the areas of telecommunications and big data networking. He received the Best Paper Award from the Network of Future Conference, in 2017.

OMER DEDEOGLU received the B.S. degree in electrical and electronics engineering from Bilkent University, in 2001, and the M.S. degree in electrical and computer engineering from New Mexico University, in 2003. He worked for R&D projects and made Radio NW investment plans at Turkcell for about six years. Since 2011, he has been working with Türk Telekom as the Radio Network Planning Expert and Manager.

YEKTA TURK (Member, IEEE) received the B.Sc. degree in electrics and electronics engineering from Anadolu University, Turkey, in 2005, the M.Sc. degree in telecommunications and computer networks from George Washington University, Washington, DC, USA, in 2007, and the Ph.D. degree from the Department of Computer Engineering, Maltepe University, Istanbul, Turkey, in 2018. He has worked in fixed and mobile network operators for ten years. He is currently a Mobile Network Architect based in Istanbul, Turkey. His research interests are in the area of mobile radio telecommunications and computer networks.